NeuroImage: Clinical 30 (2021) 102607

Contents lists available at ScienceDirect

NeuroImage: Clinical

journal homepage: www.elsevier.com/locate/ynicl

Construction and validation of a cerebral white matter hyperintensity probability map of older Koreans

Jun Sung Kim [a], Subin Lee [a], Grace Eun Kim [a], Dae Jong Oh [b], Woori Moon [b], Jong Bin Bae [b], Ji Won Han [b], Seonjeong Byun [c], Seung Wan Suh [d], Yu Yong Choi [e,f], Kyu Yeong Choi [e], Kun Ho Lee [e,g], Jae Hyoung Kim [h], Ki Woong Kim [a,b,i,*]

[a] Department of Brain and Cognitive Science, Seoul National University College of Natural Sciences, Seoul, South Korea
[b] Department of Neuropsychiatry, Seoul National University Bundang Hospital, Gyeonggido, South Korea
[c] Department of Neuropsychiatry, National Medical Center, Seoul, South Korea
[d] Department of Psychiatry, College of Medicine, Hallym University, Kangdong Sacred Heart Hospital, Seoul, South Korea
[e] National Research Center for Dementia, Chosun University, Gwangju, South Korea
[f] Biomedical Technology Center, Chosun University Hospital, Gwangju, South Korea
[g] Department of Biomedical Science, Chosun University, Gwangju, South Korea
[h] Department of Radiology, Seoul National University College of Medicine, Seoul National University Bundang Hospital, Gyeonggido, South Korea
[i] Department of Psychiatry, Seoul National University, College of Medicine, Seoul, South Korea

ARTICLE INFO

Keywords:
White matter hyperintensity
Old
Magnetic resonance image
Cerebral white matter

ABSTRACT

Background and purpose: Although two white matter hyperintensity (WMH) probability maps of healthy older adults already exist, they have several limitations in representing the distribution of WMH in healthy older adults, especially Asian older adults. We constructed and validated a WMH probability map (WPM) of healthy older Koreans and examined the age-associated differences of WMH.

Methods: We constructed WPM using development dataset that consisted of high-resolution 3D fluid-attenuated inversion recovery images of 5 age groups (60–64 years, 65–69 years, 70–74 years, 75–79 years, and 80+ years). Each age group included 30 age-matched men and women each. We tested the validity of the WPM by comparing WMH ages estimated by the WPM and the chronological ages of 30 healthy controls, 30 hypertension patients, and 30 S patients.

Results: Older age groups showed a higher volume of WMH in both hemispheres ($p < 0.001$). About 90% of the WMH were periventricular in all age groups. With advancing age, the peak of the distance histogram from the ventricular wall of the periventricular WMH shifted away from the ventricular wall, while that of deep WMH shifted toward the ventricular wall. The estimated WMH ages were comparable to the chronological ages in the healthy controls, while being higher than the chronological ages in hypertension and stroke patients.

Conclusions: This WPM may serve as a standard atlas in research on WMH of older adults, especially Asians.

1. Introduction

A probability map provides probabilistic information about the voxel-wise distribution of certain neuroanatomical or pathological structures of interest (Park et al., 2004). They have been used in various contexts to obtain information about the neuroanatomic complexity and interindividual variability within a specific population in a common stereotaxic system (Mazziotta et al., 2001, 1995). In particular, population-level lesion probability maps, in which the value at each voxel reflects the probability of finding a lesion in a specific population, can provide essential information about pathology-specific spatial variations, can be used to study differences between normal and pathological groups (Biesbroek et al., 2013; Duering et al., 2014) or detect lesions associated with neurodegenerative disorders (Toga et al., 2001).

White matter hyperintensities (WMH) are brain lesions that appear hyperintense on fluid-attenuated inversion recovery (FLAIR) magnetic resonance images (MRI). WMHs can be found in periventricular white matter (PVWMH, periventricular WMH) or within deep white matter

* Corresponding author at: Department of Neuropsychiatry, Seoul National University Bundang Hospital, 82, Gumi-ro 173beon-gil, Bundang-gu, Seongnam-si, Gyeonggi-do 13620, South Korea.
E-mail address: kwkimmd@snu.ac.kr (K.W. Kim).

https://doi.org/10.1016/j.nicl.2021.102607
Received 28 September 2020; Received in revised form 9 February 2021; Accepted 15 February 2021
Available online 4 March 2021

(DWMH), with the former being attributable to hemodynamic insufficiency (hypoperfusion) and/or cerebrospinal fluid leakage, and the latter being attributable to small vessel disease (SVD) (Fazekas et al., 1987, 1993; Kim et al., 2008). WMH are associated with various geriatric disorders (Kim et al., 2008; Mortamais et al., 2013) including major neurodegenerative diseases (Capizzano et al., 2004; Gordon et al., 2015), but they are also commonly found in healthy older adults without such disorders (de Leeuw et al., 2001; Zhuang et al., 2018). Therefore, it is not easy to distinguish between WMH that are associated with geriatric disorders and those that are associated with normal aging. This makes it difficult to interpret findings from studies that report associations between WMH and specific disorders, as it is uncertain whether the observed WMH are entirely related to the specific disorder or are a part of normal aging. In this sense, a WMH probability map (WPM) of a standard healthy normal elderly population can be a useful tool in distinguishing them without erroneous conclusion (Enzinger et al., 2006; Wen and Sachdev, 2004).

Among previously developed WPMs, all (Gordon et al., 2015; de Leeuw et al., 2001; Zhuang et al., 2018; Enzinger et al., 2006; Wen and Sachdev, 2004; Lee et al., 2016) but two (Mortamais et al., 2013; Capizzano et al., 2004) were specific to certain disease populations only. The two WPMs that were constructed from normal control populations had several limitations in terms of sample size, age, and normality of study samples. Furthermore, they were constructed from Caucasians only, signifying that they would not be applicable for use in Asian populations because the two ethnic populations are known to differ in brain shape (Lee et al., 2016) and risk of cerebrovascular diseases (Feldmann et al., 1990) and as so, a healthy normal elderly Asian population-based WPM is needed.

In this study, we constructed and validated age-stratified WPMs of healthy older Koreans and examined age-associated differences in the distribution of WMH.

2. Methods

2.1. Participants

In the development dataset for constructing WPM, we recruited 300 community-dwelling healthy Koreans aged 60 years or older from the participants of two ongoing population-based prospective cohort studies; 228 from the Korean Longitudinal Study on Cognitive Aging and Dementia (KLOSCAD) (Han et al., 2018) and 72 from the Gwangju Alzheimer's & Related Dementias (GARD) Study (Choi et al., 2019). They consisted of five age groups (60–64 years, 65–69 years, 70–74 years, 75–79 years, and 80 years or above), and each age group included 30 men and 30 age-matched women (Table 1). We diagnosed the participants as '*healthy*' when they met the following criteria: 1) The participant was functioning independently in the community without impaired activities of daily living; 2) had a Mini Mental Status Examination (MMSE) score of above −1.0 standard deviations of age-, gender-, and education adjusted norm of elderly Koreans; 3) had a Clinical Dementia Rating of 0; and 4) did not have any of the conditions, such as major psychiatric disorders including depressive disorders and substance use disorders, cognitive disorders including dementia and mild cognitive impairment, major neurologic disorders including movement disorders and strokes, cardiovascular and metabolic diseases including hypertension and diabetes mellitus, and other severe medical conditions that may influence mood and cognition.

In the validation dataset for validating the WPM, we recruited 30 healthy controls (HC), 30 cognitively normal participants with under-controlled hypertension but no stroke (HPT), and 30 cognitively normal participants who has stroke with or without hypertension (STR) from the participants of KLOSCAD. Each diagnostic group consisted of 15 men and 15 women.

All participants provided a written informed consent to participate in this study. The KLOSCAD and GARD were approved by the Institutional Review Board of the Seoul National University Bundang Hospital and the Chosun University Hospital, respectively.

2.2. Assessments

Geriatric psychiatrists or neurologists with expertise in dementia research performed face-to-face, standardized diagnostic interviews; physical and neurological examinations; laboratory tests including complete blood counts, chemistry profiles, serological tests for syphilis, echocardiography, and chest X-ray. Geriatric psychiatrists graded the severity of PVWMH and DWMH according to the Fazekas' scale (FS) (Fazekas et al., 1987). Research neuropsychologists or trained research nurses administered the CERAD-K neuropsychological assessment battery (CERAD-K-N), which consists of nine neuropsychological tests: Verbal Fluency Test, 15-item Boston Naming Test, MMSE, Word List Memory Test, Constructional Praxis Test, Word List Recall Test, Word List Recognition Test, Constructional Recall Test, and Trail Making Test A/B (Lee et al., 2004, 2002). We diagnosed dementia and other axis I mental disorders according to the diagnostic criteria of the Diagnostic and Statistical Manual of Mental Disorders, Fourth Edition, for dementia (American Psychiatric Association, 2000); and MCI according to the consensus criteria proposed by the International Working Group on MCI (Winblad et al., 2004). We defined under-controlled hypertension as having a history of hypertension but no stroke, taking antihypertensive medications but having current systolic blood pressure of ≥140 mmHg or higher or current diastolic blood pressure of ≥90 mmHg. We defined

Table 1
Characteristics of the participants included in the development dataset for constructing the white matter hyperintensity probability map.

	Age (yr)[a]							Sex[b]		
	60–64[1]	65–69[2]	70–74[3]	75–79[4]	80+[5]	p[c]	Posthoc[c]	Men	Women	p[d]
Age, yrs	62.0 ± 1.3	67.7 ± 1.2	72.1 ± 1.5	76.6 ± 1.3	83.0 ± 3.1	<0.001	1 < 2 < 3 < 4 < 5	72.5 ± 7.8	72.1 ± 7.1	0.677
Education, yrs	12.3 ± 4.7	12.4 ± 3.8	13.8 ± 3.8	12.0 ± 4.2	10.1 ± 5.0	<0.001	5 < 3	12.8 ± 4.3	11.4 ± 4.6	0.009
MMSE	27.6 ± 2.2	27.9 ± 1.5	27.6 ± 1.7	27.2 ± 1.9	26.7 ± 2.1	0.004	5 < 2	27.5 ± 1.8	27.3 ± 2.1	0.494
FS										
PVWM H	0.6 ± 0.5	0.8 ± 0.5	1.0 ± 0.6	1.3 ± 0.7	1.6 ± 0.8	<0.001	1 < 3, 4, 5; 2 < 4, 5; 3 < 5	1.1 ± 0.6	1.0 ± 0.8	0.575
DWMH	0.5 ± 0.6	0.7 ± 0.6	0.8 ± 0.7	1.1 ± 0.8	1.5 ± 0.9	<0.001	1, 2 < 4, 5; 3 < 5	0.9 ± 0.8	1.0 ± 0.8	0.348
V_{WMH}, cc	2.5 ± 2.7	4.3 ± 3.2	8.8 ± 11.4	9.8 ± 8.7	16.5 ± 17.1	<0.001	1 < 3, 4, 5; 2 < 4, 5; 3, 4 < 5	6.7 ± 8.7	10.1 ± 13.0	0.009
P_{WMH}, %	0.6 ± 0.6	1.0 ± 0.8	2.1 ± 2.7	2.4 ± 2.1	4.0 ± 4.1	<0.001	1 < 3, 4, 5; 2 < 4, 5; 3, 4 < 5	1.6 ± 2.1	2.4 ± 3.1	0.009

All values are presented as mean ± standard deviations.
MMSE, Mini Mental Status Exam; FS, Fazekas' scale; PVWMH, periventricular white matter hyperintensity; DWMH, deep white matter hyperintensity; V_{WMH}, total volume of white matter hyperintensity; P_{WMH}, proportion of total white matter hyperintensity in total brain white matter.
[a] Each age group includes 30 men and 30 age-matched women.
[b] Each sex group includes 30 from each age group.
[c] One-way analysis of variance with Bonferroni posthoc comparisons.
[d] Student *t*-test.

stroke as having a history of stroke regardless of residual symptoms.

2.3. Acquisition of brain magnetic resonance imaging (MRI)

We obtained high-resolution 3D T1 and FLAIR images for developing the WPM. In the KLOSCAD, all images were obtained from a 3.0 Tesla Achieva Scanner (Philips Medical Systems; Eindhoven, NL) using the following protocol, T1: acquired voxel size = 1.0 mm × 0.5 mm × 0.5 mm, echo time = 4.6 ms, repetition time = 8.1 ms, acquisition axial plane matrix size = 240 mm × 240 mm, number of excitation = 1, flip angle = 8°, inversion time = not applied and FLAIR: acquired voxel size = 0.47 mm × 0.47 mm × 3.0 mm, slice thickness = 3 mm, spacing between slices = 3 mm, echo time = 125 ms, repetition time = 9900 ms, acquisition axial plane matrix size = 256 mm × 256 mm, number of excitations = 1, flip angle = 90°, and inversion time = 2800 ms. In the GARD, all images were obtained from the 3.0 Tesla Skyra Scanner (SIEMENS Healthineers; Erlangen, DE) using the following protocol, T1: acquired voxel size = 0.8 mm × 0.8 mm × 0.8 mm, echo time = 2.14 ms, repetition time = 2.3 ms, acquisition sagittal plane matrix size = 320 mm × 320 mm, number of excitations = 1, flip angle = 9°, inversion time = 900 ms and FLAIR: acquired voxel size = 0.63 mm × 0.63 mm × 7.5 mm, slice thickness = 5 mm, spacing between slices = 7.5 mm, echo time = 96 ms, repetition time = 8000 ms, acquisition axial plane matrix size = 218 mm × 384 mm, number of excitations = 1, flip angle = 150°, and inversion time = 2500 ms.

2.4. Construction of WPM

We conducted all image preprocessing and registration using the Statistical Parametric Mapping software (version 8, SPM8; Wellcome Trust Centre for Neuroimaging, London). First, we spatially normalized each individual's T1 image to a previously developed standard template for Korean normal elderly (KNE200 template) (Lee et al., 2016). The normalization process involves estimating an optimum 12-parameter affine transformation that matches the head orientation of the individual image to the template, followed by estimating a nonlinear deformation which further minimizes the residual squared difference between the individual image and the template (Ashburner et al., 2012). Through normalization to a common stereotaxic space (voxel size 1 × 1 × 1 mm, slice thickness 1 mm), we aimed to correct for inter-individual differences in brain size and shape. Meanwhile, we applied bias correction on the FLAIR images to correct for non-uniformities caused by the bias field due to different tissue properties and physics of MR scanning, using the 'Segment' tool from SPM8. The bias correction method in SPM8 uses a Bayesian model to accurately estimate a smooth function that is multiplied with the image using prior knowledge about field distributions likely to be encountered (Ashburner and Friston, 2005). Next, we coregistered the bias corrected FLAIR images to native T1 images. We then applied the transformation parameters produced from the normalization step of T1 images to the bias corrected, T1-coregistered FLAIR images to produce spatially KNE-normalized FLAIR images.

We segmented WMH from the spatially KNE-normalized FLAIR images by using a fully automated in-house code run on MATLAB 2014a (MATLAB and statistics Toolbox Release 2014a, MathWorks, Inc., Natick, MA) which has been previously shown to work on different protocols from different scanners without any parameter adjustment (Yoo et al., 2014). The resulting WMH images consist of values of 1 or 0, reflecting the presence or absence, respectively, of WMH in each voxel. We then overlapped the segmented WMH images to cumulatively add the voxel values and divided by the total number of WMH images, creating a map that represent the probability of finding a WMH in each voxel. To reduce noise associated with individual anatomical details or other imaging artifacts, we applied smoothing with a Gaussian filter with a FWHM of 1 (Warntjes et al., 2013) and excluded WPM voxels with a value of 0.10 or less (Yoshita et al., 2005). The final WPM, constructed for each age group, are shown in Fig. 1.

2.5. Validation of WPM

To validate the WPM, we first validated the constructed WPMs with WMH of the HC group. We calculated the WMH age of each participant using the WPM. We calculated the deviance of WMH of each participant from the five age-specific WPMs. First, we prepared individual's WMH image and five WPMs for every participant. We overlaid WMH and each of the five WPMs, one at a time. Then we subtracted WMH's voxel value (0 and 1, reflecting absence and presence, respectively) from WPM's voxel values (0–1). We took the absolute values of the subtracted values from each voxel and summed all the values. We then divided the sum by the total number of voxels in the image to calculate the average deviances (Heinrich et al., 2012). We assigned the WPM age group with the lowest average deviance as their WMH-estimated age group.

Though WMH occurs in normal aging, it is known to be associated with various diseases such as hypertension and stroke (Bokura et al., 2006; Dufouil et al., 2001). Since these two diseases are known risk groups of WMH, we demonstrated the validity and applicability of our WPMs by verifying the hypothesis that these groups will have higher WMH age than a healthy group. We calculated WPM-estimated WMH-ages of HPT and STR groups with the same procedures we applied on HC group. We compared the WPM-estimated WMH-ages with the chronological ages of the participants in each diagnostic group (HC, HPT and STR) using chi-square goodness of fit tests. We then coded both the five chronological age groups and WMH age groups (60–64, 65–69, 70–74, 75–79, 80+) as 1, 2, 3, 4, and 5. We subtracted the individual's WMH age code from their chronological age code to get a continuous value. We input this continuous value into a ROC analysis and calculated the area under the curve. We performed this analysis separately for HC vs HPT, HC vs STR, and HC vs HPT and STR.

We also investigated average WMH probability at each distance away from the ventricle. We first calculated the total number of white matter voxels at each distance from the ventricle (in intervals of 1 mm). We then summed all the WPM voxel values at each distance from the ventricle. We then divided the sum of the WPM voxel values by the total number of white matter voxels at each distance from the ventricle. The distance-wise WMH probability histograms were constructed for whole WMH, PVWMH, and DWMH separately and are shown in Fig. 2. We determined which WMH voxels correspond to PVWMH and DWMH according to the 'continuity to ventricle' rule (Fazekas et al., 1987).

2.6. Statistical analyses

For all statistical analyses, we used SPSS for Windows version 20.0 (IBM Co., Armonk, NY, USA), and considered a two-sided p-value less than 0.05 as statistically significant. We compared continuous variables using independent samples t-test or analysis of variance (ANOVA), and categorical variables using chi-squared test.

For each of the total WMH, PVWMH, and DWMH, we calculated the total volume, hemispheric volume, and regional volumes and proportions. We obtained hemispheric volumes by dividing the WMH labels into those corresponding to the left and right hemispheres by referencing the longitudinal fissure, and anterior and posterior regions as specified in a white matter atlas proposed by Murray et al. (2010).

For all analyses, we used SPSS for Windows version 20.0 (IBM Co., Armonk, NY, USA), and considered a two-sided p-value less than 0.05 as statistically significant.

3. Results

In the development dataset, the participants were 72.3 ± 7.5 years old and 12.1 ± 4.5 years educated on average. Compared to the male participants, female participants showed a higher volume and proportion of WMH (p = 0.009), but comparable FS scores, age, and MMSE

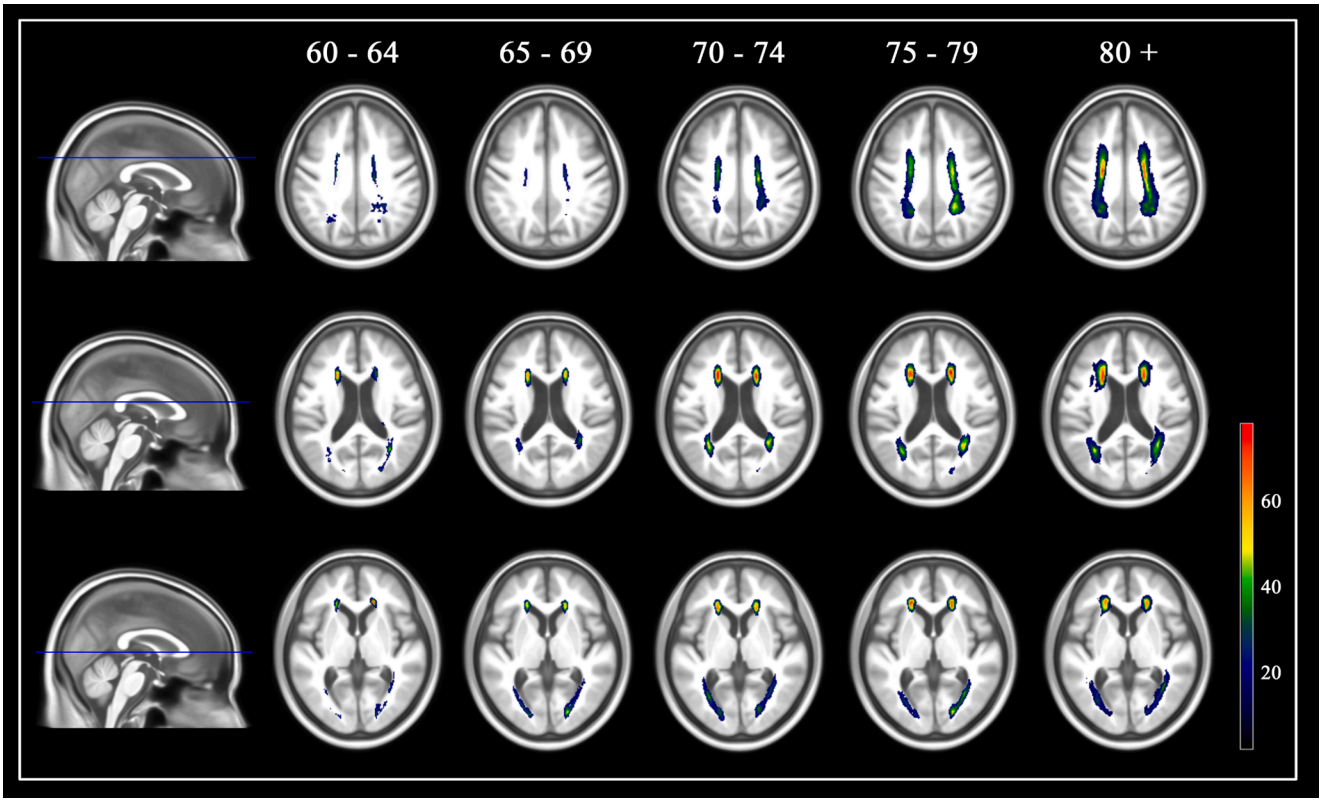

Fig. 1. White matter hyperintensity probability map of the levels of centrum semiovale, corona radiata, and striatocapsular region.

scores. The older the group of participants, the higher the FS score and volume and proportion of the WMH ($p < 0.001$). The volume of WMH in the 80+ group was more than six folds higher than that in the 60–64 age group (Table 1). These age-associated differences in the volume and proportion of the WMH were observed in both hemispheres ($p < 0.001$) and regions ($p < 0.001$, Supplementary Table S1). The ratios of the hemispheric WMH volumes and proportions between right and left hemispheres and those of regional WMH volumes and proportions between anterior and posterior regions were comparable in all the age groups (Supplementary Table S1).

Fig. 1 demonstrated the constructed WPM in three representative brain slices, including the centrum semiovale, corona radiata, and striatocapsular region. The volume and proportion of the PVWMH were far larger than those of the DWMH in all age groups in both hemispheres and regions ($p < 0.001$), indicating that the age-associated increase of total WMH may be mainly attributable to that of PVWMH. In the distance histogram from the ventricular wall of WMH (Fig. 2), nearly 90% of WMH were located within 30 mm from the ventricle in all the age groups. However, the peak of the distance histogram shifted to the right with advancing age from 2 mm in the 60–64 age group to 10 mm in the 80+ age group. When we analyzed the distance histograms of PVWMH and DWMH separately, the peak of PVWMH shifted away from the ventricular wall while that of DWMH shifted towards the ventricular wall with advancing age.

In the validation dataset, age, sex, and MMSE scores were comparable between the three diagnostic groups. Though WMH volume trendily increased in order of HC, HPT and STR groups, the difference in WMH volume between the STR and, HC and HPT groups was statistically significant in posthoc comparisons (Table 2). As summarized in Table 3, the estimated WMH ages were comparable to the chronological ages in the HC group ($X^2 = 0.768$, $p = 0.857$), while higher than the chronological ages in both the HPT and STR groups ($X^2 = 88.949$, $p < 0.001$ for the HPT group; $X^2 = 246.178$, $p < 0.001$ for the STR group). The WPM discriminated HPT and STR, from HC group (AUC = 0.722, $p = 0.001$), and HPT (AUC = 0.727, $p = 0.003$) and STR (AUC = 0.717, $p = 0.004$) groups from HC group, separately. Compared to the WPM, the HPT and STR groups showed a higher volume of total WMH, PVWMH and DWMH in all regions ($p < 0.001$) and higher proportion of total WMH and PVWMH ($p < 0.001$) except right hemisphere and posterior region of PVWMH. Though proportion of DWMH in whole brain region was significantly different between WPM, and HPT and STR ($p < 0.001$), proportion in other regions were comparable between groups (Supplementary Table S2).

4. Discussion

In this study, we constructed a WPM using 3.0 T FLAIR MR Images of community-dwelling healthy elderly Koreans and showed its validity by comparing the chronological ages with the WMH ages estimated by the WPM in an independent validation dataset.

As far as we know, our WPM is the first that comes from an Asian population and covers the entire age range of older adults from 60 years and above. Furthermore, we strictly balanced gender and age ratios of the sample and rigorously excluded the conditions that could have influenced the risk and distribution of the WMH from the sample. Although several studies reported WPMs (Enzinger et al., 2006; Wen and Sachdev, 2004; Charil et al., 2003; Damulina et al., 2019; DeCarli et al., 2005; Lee et al., 1999; Narayanan et al., 1997; Ryu et al., 2014), most of them were disease-specific WPMs, such as the cerebrovascular disease WPMs (Charil et al., 2003; Lee et al., 1999; Ryu et al., 2014) or Alzheimer's disease WPMs (Damulina et al., 2019; DeCarli et al., 2005). There were two WPMs of healthy older adults; one from the Austrian Stroke Prevention Study (ASPS) using proton density weighted images (Enzinger et al., 2006) and the other from the Path Through Life (PTL) project using FLAIR images (Wen and Sachdev, 2004). The ASPS WPM was constructed from 189 community-dwelling volunteers (95 men and 94 women) aged 50–75 years (mean = 60.8, standard deviation = 6.2) without neuropsychiatric disorders. The PTL WPM was constructed from

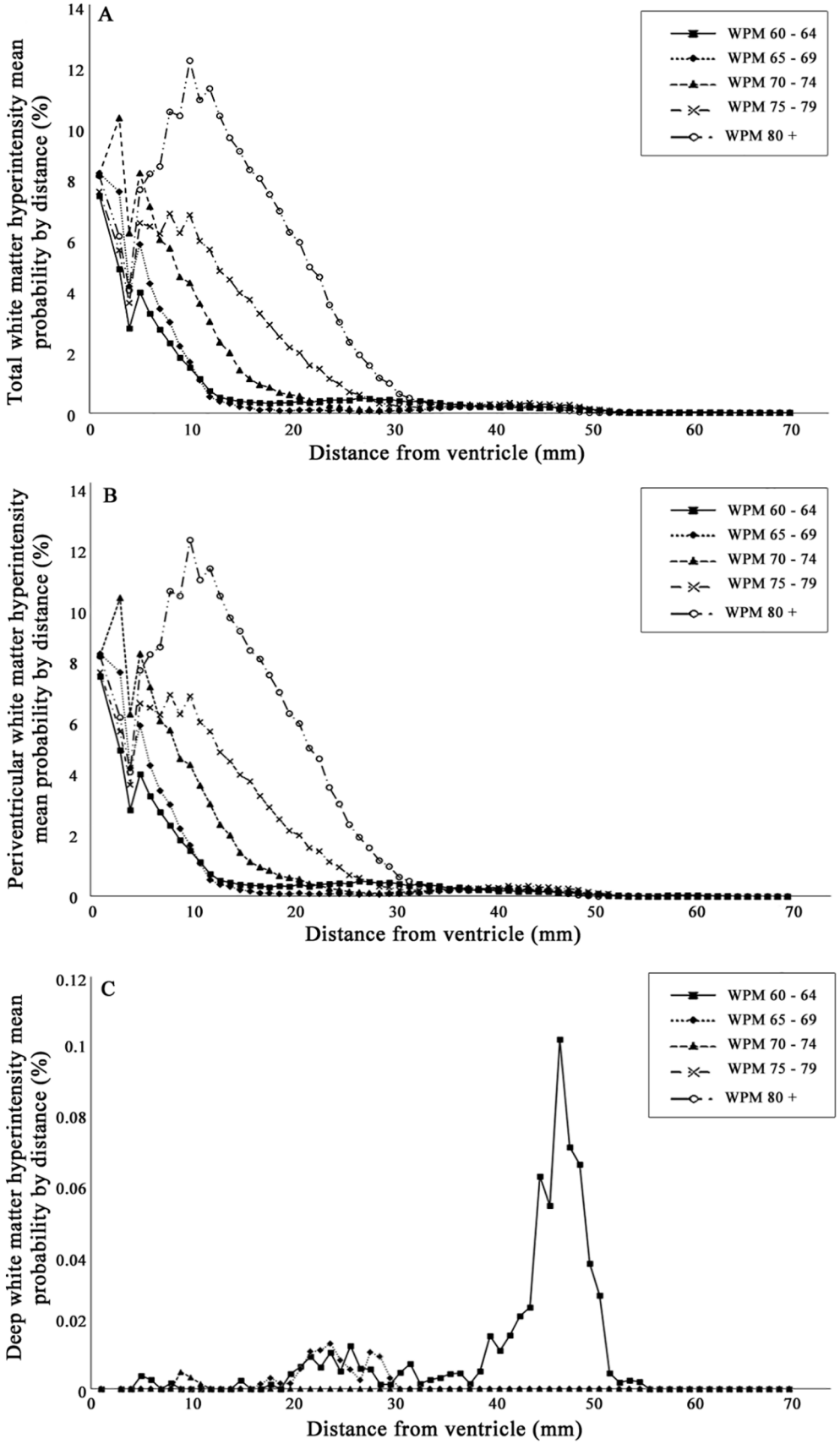

Fig. 2. Distance histogram from the ventricular wall of white matter hyperintensity. (A) Total white matter hyperintensity, (B) periventricular white matter hyperintensity, and (C) deep white matter hyperintensity.

Table 2
Characteristics of the participants included in the dataset for validating the whit matter hyperintensity probability map.

	HC[1]	HPT[2]	STR[3]	p[a]	Posthoc
Age, yrs	69.1 ± 5.7	69.1 ± 5.8	69.5 ± 6.4	0.948	–
Education, yrs	10.0 ± 4.0	12.8 ± 3.3	11.8 ± 4.1	0.021	1 < 2
MMSE	28.0 ± 1.7	27.7 ± 1.4	27.7 ± 1.6	0.626	–
FS					
PVWMH	0.6 ± 0.5	0.9 ± 0.7	1.3 ± 0.5	<0.001	1 < 3
DWMH	0.4 ± 0.5	0.7 ± 0.5	1.3 ± 0.5	<0.001	1 < 3
V_{WMH}, cc	8.7 ± 4.6	15.9 ± 9.8	24.8 ± 17.5	<0.001	1, 2 < 3
P_{WMH}, %	2.1 ± 1.1	3.8 ± 2.4	6.0 ± 4.2	<0.001	1, 2 < 3

All values are presented as mean ± standard deviations.
HC, cognitively normal participants without hypertension and stroke; HPT, cognitively normal participants with hypertension but no stroke; STR, cognitively normal participants with stroke; MMSE, Mini Mental Status Exam; FS, Fazekas' scale; PVWMH, periventricular white matter hyperintensity; DWMH, deep white matter hyperintensity; V_{WMH}, total volume of white matter hyperintensity; P_{WMH}, proportion of total white matter hyperintensity in total brain white matter.
[a] One-way analysis of variance for continuous variables and chi-square test for categorical variables with Bonferroni posthoc comparisons.

Table 3
Comparisons between the chronological ages and the estimated white matter hyperintensity ages by the white matter hyperintensity probability map in the validation dataset.

A		Estimated white matter hyperintensity age				
		60–64	65–69	70–74	75–79	80+
Chronological age	60–64	7	1	0	0	0
	65–69	3	5	0	0	0
	70–74	0	1	6	0	0
	75–79	0	0	1	6	0
	80+	0	0	0	0	0
B		Estimated white matter hyperintensity age				
		60–64	65–69	70–74	75–79	80+
Chronological age	60–64	3	3	2	0	0
	65–69	1	2	4	1	0
	70–74	0	0	3	4	0
	75–79	0	0	1	3	3
	80+	0	0	0	0	0
C		Estimated white matter hyperintensity age				
		60–64	65–69	70–74	75–79	80+
Chronological age	60–64	4	1	3	1	0
	65–69	0	1	3	1	0
	70–74	0	0	3	4	0
	75–79	0	0	0	4	5
	80+	0	0	0	0	0

A, cognitively normal participants without hypertension and stroke; B, cognitively normal participants with hypertension but no stroke; C, cognitively normal participants with stroke.
Values are the numbers of participants.

477 randomly selected healthy residents (251 men and 226 women) aged 60–64 (mean = 62.6, standard deviation = 1.5). However, these WPMs had some limitations to represent the probability of WMH in healthy older adults; the ASPS WPM was constructed from a small number of subjects and the PTL WPM was constructed from subjects in their early 60 s only, and did not exclude the subjects with a history of stroke, head injury, epilepsy, and heart disease. Furthermore, both WPMs may not be directly applicable to Asians because they were constructed from Caucasians only, since the brain shape (Lee et al., 2016) and the risk of cerebrovascular diseases and WMH are different between Caucasians and Asians (Feldmann et al., 1990). Volume of the WMH in the current sample was smaller than that reported in the previous studies on healthy older Caucasians (Kaskikallio et al., 2020; Raz et al., 2012).

In our WPM, the probability of WMH increased continuously with advancing age. The prevalence and severity of WMH have been consistently reported to increase with age regardless of ethnicities (Liao et al., 1997; Zhuang et al., 2018). Across the human lifespan, cerebral metabolic rates for oxygen and glucose decreased by approximately 6% per decade (Petit-Taboue et al., 1998) and cerebral blood flow decreased by 4.8 mL/min per year (Buijs et al., 1998). The reduction in cerebral metabolic rates was coupled to the concurrent hemodynamic insufficiency (Akiyama et al., 1997; Leenders et al., 1990). In addition, atrial fibrillation (de Leeuw et al., 2000) and carotid atherosclerosis (Yin et al., 2012) became more prevalent with advancing age. All these age-associated changes may contribute to the development and progression of cerebral WMH with advancing age in late life. Considering the regional WM volumes, our WPM shows that WPM progresses more in the anterior region with advancing age than in the posterior region. We assigned the frontal lobe as the anterior region and the parietal, occipital, and temporal lobes as the posterior region, according to the WM atlas proposed by Murray et al. (2010). de Bresser et al. examined the lobar distribution of WMH in 60 older adults with diabetes and their 54 matched controls, and found that the majority of WMH were present in the frontal region, followed by the parietal, temporal, and occipital regions in both groups (de Bresser et al., 2018). The reason why WMH are more common in frontal regions compared to other regions may be due to the chronic ischemia resulting from the sclerosis of penetrating arteries that are longest in the WM regions around the frontal horns and head of the caudate nuclei (Ishii et al., 1986).

As shown in the distance histogram (Fig. 2), the first peaks of WMH appeared within 3 mm from the ventricular wall, followed by the second peaks between 5 and 12 mm from the ventricular wall, and the first and second peaks were clearly separated by dipping points at 4 mm from the ventricular wall in all the age groups. These results support our previous proposal to classify WMH using the 'distance from ventricle' rule instead of the 'continuity to ventricle' rule. We proposed to classify WMH into 4 groups using the distance from the ventricle surface: juxtaventricular WMH (JVWMH); non-ischemic WMH within 3 mm from the ventricle, directly contiguous to the ventricular surface, and mainly attributable to cerebrospinal fluid leakage; PVWMH, ischemic WMH located in the range from 3 mm to 13 mm from the ventricular surface where the periventricular watershed area is located and attributable to hypoperfusion; DWMH, ischemic WMH located between PVWMH and juxtacortical WMH (JCWMH) and mainly due to SVD; JCWMH, ischemic WMH located within 4 mm from the corticomedullary junction, which may have a different vascular etiology from DWMH because it has a dual blood supply in this region (Kim et al., 2008). In semi-quantitative visual classification of WMH, WMH are usually classified into PVWMH and DWMH using the 'continuity to ventricle' rule. However, this classification may not properly reflect the etiological and pathological differences of WMH by their locations (Fazekas et al., 1993; Kim et al., 2008; Wen and Sachdev, 2004). First of all, the continuity to ventricle does not have anatomical ground for assuming etiological differences of WMH. In addition, PVWMH and DWMH are more likely to merge as their volumes increase in a given volume of brain. In our distance histograms of WMH, as the WMH volume increased with advancing age, the peaks of the distance histogram of WMH and PVWMH shifted away from the ventricular wall, while the peak of the distance histogram of DWMH shifted to the ventricular wall (Fig. 2).

In the validation dataset, the WMH age estimated using our WPM was comparable to the chronological age in the HC group, indicating that our WPM validly represent the distribution of WMH in healthy older adults. In contrast, the WMH age estimated using our WPM was older than the chronological age in the HPT and STR groups, which further supported the validity of our WPM. Hypertension is known to increase WMH (Dufouil et al., 2001; Kim et al., 2020; Liao et al., 1997) by inducing both hemodynamic insufficiency due to increasing vascular resistance and disturbed hemodynamic flow (Choi et al., 2015; O'Rourke and Hashimoto, 2007). SVD also increases WMH (Bokura

et al., 2006; Vermeer et al., 2003) by causing endothelial dysfunction of cerebral vessels (Cuadrado-Godia et al., 2018).

This study has a couple of limitations. First, the differences between age groups may not necessarily indicate the age-associated changes because this study employed a cross-sectional design. Second, our WMP may not be directly applicable to the population of different ethnicities like Caucasians and/or living in different geographic regions because brain shape is different between ethnic groups (Lee et al., 2016) and the risk of WMH is also different between ethnic groups and/or geographic regions with different lifestyles and environments (Divers et al., 2013; Gow et al., 2012). Third, although we tried to compensate for differences in resolution of the images by normalizing them to a common template, pooling MR images from two different scanners and protocols might influence the accuracy for the measurement (Schnack et al., 2004). Particularly, the difference in slice thickness might cause the different capacity of detecting small lesion (Bradley and Glenn, 1987).

5. Summary/conclusions

We successfully constructed and validated a WPM from a large, well-balanced sample of healthy elderly Koreans. The constructed WPMs can strongly provide a tool to study WMH distribution in both pathology and normal aging; moreover, it can provide an indirect clue regarding the WMH development; thus, the WPMs may serve as a prominent atlas of the age-related distribution of WMH.

CRediT authorship contribution statement

Jun Sung Kim: Conceptualization, Methodology, Validation, Formal analysis, Investigation, Writing - original draft, Writing - review & editing, Visualization. **Subin Lee:** Methodology, Software, Writing - review & editing. **Grace Eun Kim:** Methodology. **Dae Jong Oh:** Resources. **Woori Moon:** Resources. **Jong Bin Bae:** Resources. **Ji Won Han:** Resources, Writing - review & editing. **Seonjeong Byun:** Resources. **Seung Wan Suh:** Resources. **Yu Yong Choi:** Resources. **Kyu Yeong Choi:** Resources. **Kun Ho Lee:** Resources. **Jae Hyoung Kim:** Resources. **Ki Woong Kim:** Conceptualization, Writing - original draft, Writing - review & editing, Supervision, Project administration.

Declaration of Competing Interest

The authors declare that they have no known competing financial interests or personal relationships that could have appeared to influence the work reported in this paper.

Acknowledgments

This study was supported by a grant from the Research of Korea Centers for Disease Control and Prevention (grant no. 2019-ER6201-00) and Institute for Information & communications Technology Promotion (IITP) grant funded by the Korea government (MSIT) (2018-0-00861, Intelligent SW Technology Development for Medical Data Analysis).

Ethical approval

All procedures performed in studies involving human participants were in accordance with the ethical standards of the institutional and/or national research committee and with the 1964 Helsinki declaration and its later amendments or comparable ethical standards.

Informed consent

Informed consent was obtained from all individual participants included in the study.

Appendix A. Supplementary data

Supplementary data to this article can be found online at https://doi.org/10.1016/j.nicl.2021.102607.

References

Akiyama, H., Meyer, J.S., Mortel, K.F., Terayama, Y., Thornby, J.I., Konno, S., 1997. Normal human aging: factors contributing to cerebral atrophy. J. Neurol. Sci. 152 (1), 39–49. https://doi.org/10.1016/s0022-510x(97)00141-x.

American Psychiatric Association, 2000. DSM-IV-TR: Diagnostic and Statistical Manual of Mental Disorders, Text Revision. American Psychiatric Association, Washington DC.

Ashburner, J., Barnes, G., Chen, C., Daunizeau, J., Flandin, G., Friston, K., et al., 2012. SPM8 Manual. Functional Imaging Laboratory, Institute of Neurology.

Ashburner, J., Friston, K.J., 2005. Unified segmentation. Neuroimage 26 (3), 839–851. https://doi.org/10.1016/j.neuroimage.2005.02.018.

Biesbroek, J.M., Kuijf, H.J., van der Graaf, Y., Vincken, K.L., Postma, A., Mali, W.P., et al., 2013. Association between subcortical vascular lesion location and cognition: a voxel-based and tract-based lesion-symptom mapping study. The SMART-MR study. PLoS One 8 (4), e60541. https://doi.org/10.1371/journal.pone.0060541.

Bokura, H., Kobayashi, S., Yamaguchi, S., Iijima, K., Nagai, A., Toyoda, G., et al., 2006. Silent brain infarction and subcortical white matter lesions increase the risk of stroke and mortality: a prospective cohort study. J. Stroke Cerebrovasc. Dis. 15 (2), 57–63. https://doi.org/10.1016/j.jstrokecerebrovasdis.2005.11.001.

Bradley, W.G., Glenn, B.J., 1987. The effect of variation in slice thickness and interslice gap on MR lesion detection. AJNR Am. J. Neuroradiol. 8 (6), 1057–1062.

Buijs, P.C., Krabbe-Hartkamp, M.J., Bakker, C.J., de Lange, E.E., Ramos, L.M., Breteler, M.M., et al., 1998. Effect of age on cerebral blood flow: measurement with ungated two-dimensional phase-contrast MR angiography in 250 adults. Radiology 209 (3), 667–674. https://doi.org/10.1148/radiology.209.3.9844657.

Capizzano, A.A., Acion, L., Bekinschtein, T., Furman, M., Gomila, H., Martinez, A., et al., 2004. White matter hyperintensities are significantly associated with cortical atrophy in Alzheimer's disease. J. Neurol. Neurosurg. Psychiatry 75 (6), 822–827. https://doi.org/10.1136/jnnp.2003.019273.

Charil, A., Zijdenbos, A.P., Taylor, J., Boelman, C., Worsley, K.J., Evans, A.C., et al., 2003. Statistical mapping analysis of lesion location and neurological disability in multiple sclerosis: application to 452 patient data sets. Neuroimage 19 (3), 532–544. https://doi.org/10.1016/S1053-8119(03)00117-4.

Choi, J.Y., Cui, Y., Kim, B.G., 2015. Interaction between hypertension and cerebral hypoperfusion in the development of cognitive dysfunction and white matter pathology in rats. Neuroscience 303, 115–125. https://doi.org/10.1016/j.neuroscience.2015.06.056.

Choi, K.Y., Lee, J.J., Gunasekaran, T.I., Kang, S., Lee, W., Jeong, J., et al., 2019. APOE promoter polymorphism-219T/G is an effect modifier of the influence of APOE epsilon4 on Alzheimer's disease risk in a multiracial sample. J. Clin. Med. 8 (8) https://doi.org/10.3390/jcm8081236.

Cuadrado-Godia, E., Dwivedi, P., Sharma, S., Ois Santiago, A., Roquer Gonzalez, J., Balcells, M., et al., 2018. Cerebral small vessel disease: a review focusing on pathophysiology, biomarkers, and machine learning strategies. J. Stroke 20 (3), 302–320. https://doi.org/10.5853/jos.2017.02922.

Damulina, A., Pirpamer, L., Seiler, S., Benke, T., Dal-Bianco, P., Ransmayr, G., et al., 2019. White matter hyperintensities in Alzheimer's disease: a lesion probability mapping study. J. Alzheimers Dis. 68 (2), 789–796. https://doi.org/10.3233/JAD-180982.

de Bresser, J., Kuijf, H.J., Zaanen, K., Viergever, M.A., Hendrikse, J., Biessels, G.J., et al., 2018. White matter hyperintensity shape and location feature analysis on brain MRI; proof of principle study in patients with diabetes. Sci. Rep. 8 (1), 1893. https://doi.org/10.1038/s41598-018-20084-y.

de Leeuw, F.E., de Groot, J.C., Oudkerk, M., Kors, J.A., Hofman, A., van Gijn, J., et al., 2000. Atrial fibrillation and the risk of cerebral white matter lesions. Neurology 54 (9), 1795–1801. https://doi.org/10.1212/WNL.54.9.1795.

de Leeuw, F.E., de Groot, J.C., Achten, E., Oudkerk, M., Ramos, L.M., Heijboer, R., et al., 2001. Prevalence of cerebral white matter lesions in elderly people: a population based magnetic resonance imaging study. The Rotterdam Scan Study. J. Neurol. Neurosurg. Psychiatry 70 (1), 9–14. https://doi.org/10.1136/jnnp.70.1.9.

DeCarli, C., Fletcher, E., Ramey, V., Harvey, D., Jagust, W.J., 2005. Anatomical mapping of white matter hyperintensities (WMH): exploring the relationships between periventricular WMH, deep WMH, and total WMH burden. Stroke 36 (1), 50–55. https://doi.org/10.1161/01.STR.0000150668.58689.f2.

Divers, J., Hugenschmidt, C., Sink, K.M., Williamson, J.D., Ge, Y., Smith, S.C., et al., 2013. Cerebral white matter hyperintensity in African Americans and European Americans with type 2 diabetes. J. Stroke Cerebrovasc. Dis. 22 (7), e46–e52. https://doi.org/10.1016/j.jstrokecerebrovasdis.2012.03.019.

Duering, M., Gesierich, B., Seiler, S., Pirpamer, L., Gonik, M., Hofer, E., et al., 2014. Strategic white matter tracts for processing speed deficits in age-related small vessel disease. Neurology 82 (22), 1946–1950. https://doi.org/10.1212/WNL.0000000000000475.

Dufouil, C., de Kersaint-Gilly, A., Besancon, V., Levy, C., Auffray, E., Brunnereau, L., et al., 2001. Longitudinal study of blood pressure and white matter hyperintensities: the EVA MRI Cohort. Neurology 56 (7), 921–926. https://doi.org/10.1212/WNL.56.7.921.

Enzinger, C., Smith, S., Fazekas, F., Drevin, G., Ropele, S., Nichols, T., et al., 2006. Lesion probability maps of white matter hyperintensities in elderly individuals: results of

the Austrian stroke prevention study. J. Neurol. 253 (8), 1064–1070. https://doi.org/10.1007/s00415-006-0164-5.
Fazekas, F., Chawluk, J.B., Alavi, A., Hurtig, H.I., Zimmerman, R.A., 1987. MR signal abnormalities at 1.5 T in Alzheimer's dementia and normal aging. AJR Am. J. Roentgenol. 149 (2), 351–356. https://doi.org/10.2214/ajr.149.2.351.
Fazekas, F., Kleinert, R., Offenbacher, H., Schmidt, R., Kleinert, G., Payer, F., et al., 1993. Pathologic correlates of incidental MRI white matter signal hyperintensities. Neurology 43 (9), 1683–1689. https://doi.org/10.1212/WNL.43.9.1683.
Feldmann, E., Daneault, N., Kwan, E., Ho, K.J., Pessin, M.S., Langenberg, P., et al., 1990. Chinese-white differences in the distribution of occlusive cerebrovascular disease. Neurology 40 (10), 1540–1545. https://doi.org/10.1212/WNL.40.10.1540.
Gordon, B.A., Najmi, S., Hsu, P., Roe, C.M., Morris, J.C., Benzinger, T.L., 2015. The effects of white matter hyperintensities and amyloid deposition on Alzheimer dementia. Neuroimage Clin. 8, 246–252. https://doi.org/10.1016/j.nicl.2015.04.017.
Gow, A.J., Bastin, M.E., Munoz Maniega, S., Valdes Hernandez, M.C., Morris, Z., Murray, C., et al., 2012. Neuroprotective lifestyles and the aging brain: activity, atrophy, and white matter integrity. Neurology 79 (17), 1802–1808. https://doi.org/10.1212/WNL.0b013e3182703fd2.
Han, J.W., Kim, T.H., Kwak, K.P., Kim, K., Kim, B.J., Kim, S.G., et al., 2018. Overview of the Korean longitudinal study on cognitive aging and dementia. Psychiatry Investig. 15 (8), 767–774. https://doi.org/10.30773/pi.2018.06.02.
Heinrich, M.P., Jenkinson, M., Bhushan, M., Matin, T., Gleeson, F.V., Brady, S.M., et al., 2012. MIND: modality independent neighbourhood descriptor for multi-modal deformable registration. Med Image Anal. 16 (7), 1423–1435. https://doi.org/10.1016/j.media.2012.05.008.
Ishii, N., Nishihara, Y., Imamura, T., 1986. Why do frontal lobe symptoms predominate in vascular dementia with lacunes? Neurology 36 (3), 340–345. https://doi.org/10.1212/wnl.36.3.340.
Kaskikallio, A., Karrasch, M., Koikkalainen, J., Lotjonen, J., Rinne, J.O., Tuokkola, T., et al., 2020. White matter hyperintensities and cognitive impairment in healthy and pathological aging: a quantified brain MRI study. Dement. Geriatr. Cogn. Disord. 48 (5–6), 297–307. https://doi.org/10.1159/000506124.
Kim, J.S., Lee, S., Suh, S.W., Bae, J.B., Han, J.H., Byun, S., et al., 2020. Association of low blood pressure with white matter hyperintensities in elderly individuals with controlled hypertension. J. Stroke 22 (1), 99–107. https://doi.org/10.5853/jos.2019.01844.
Kim, K.W., MacFall, J.R., Payne, M.E., 2008. Classification of white matter lesions on magnetic resonance imaging in elderly persons. Biol. Psychiatry 64 (4), 273–280. https://doi.org/10.1016/j.biopsych.2008.03.024.
Lee, J.H., Lee, K.U., Lee, D.Y., Kim, K.W., Jhoo, J.H., Kim, J.H., et al., 2002. Development of the Korean Version of the Consortium to establish a registry for Alzheimer's disease assessment packet (CERAD-K) clinical and neuropsychological assessment batteries. J. Gerontol. Ser. B: Psychol. Sci. Soc. Sci. 57 (1), P47–P53.
Lee, D.Y., Lee, K.U., Lee, J.H., Kim, K.W., Jhoo, J.H., Kim, S.Y., et al., 2004. A normative study of the CERAD neuropsychological assessment battery in the Korean elderly. J. Int. Neuropsychol. Soc. 10 (1), 72–81.
Lee, M.A., Smith, S., Palace, J., Narayanan, S., Silver, N., Minicucci, L., et al., 1999. Spatial mapping of T2 and gadolinium-enhancing T1 lesion volumes in multiple sclerosis: evidence for distinct mechanisms of lesion genesis? Brain 122 (7), 1261–1270. https://doi.org/10.1093/brain/122.7.1261.
Lee, H., Yoo, B.I., Han, J.W., Lee, J.J., Oh, S.Y., Lee, E.Y., et al., 2016. Construction and Validation of brain MRI templates from a Korean normal elderly population. Psychiatry Investig. 13 (1), 135–145. https://doi.org/10.4306/pi.2016.13.1.135.
Leenders, K.L., Perani, D., Lammertsma, A.A., Heather, J.D., Buckingham, P., Healy, M. J., et al., 1990. Cerebral blood flow, blood volume and oxygen utilization. Normal values and effect of age. Brain 113 (Pt 1), 27–47. https://doi.org/10.1093/brain/113.1.27.
Liao, D., Cooper, L., Cai, J., Toole, J., Bryan, N., Burke, G., et al., 1997. The prevalence and severity of white matter lesions, their relationship with age, ethnicity, gender, and cardiovascular disease risk factors: the ARIC Study. Neuroepidemiology 16 (3), 149–162. https://doi.org/10.1159/000368814.
Mazziotta, J.C., Toga, A.W., Evans, A., Fox, P., Lancaster, J., 1995. A probabilistic atlas of the human brain: theory and rationale for its development. The International Consortium for Brain Mapping (ICBM). Neuroimage 2 (2), 89–101. https://doi.org/10.1006/nimg.1995.1012.
Mazziotta, J., Toga, A., Evans, A., Fox, P., Lancaster, J., Zilles, K., et al., 2001. A probabilistic atlas and reference system for the human brain: International Consortium for Brain Mapping (ICBM). Philos. Trans. R. Soc. Lond. B Biol. Sci. 356 (1412), 1293–1322. https://doi.org/10.1098/rstb.2001.0915.
Mortamais, M., Artero, S., Ritchie, K., 2013. Cerebral white matter hyperintensities in the prediction of cognitive decline and incident dementia. Int. Rev. Psychiatry 25 (6), 686–698. https://doi.org/10.3109/09540261.2013.838151.
Murray, M.E., Senjem, M.L., Petersen, R.C., Hollman, J.H., Preboske, G.M., Weigand, S. D., et al., 2010. Functional impact of white matter hyperintensities in cognitively normal elderly subjects. Arch. Neurol. 67 (11), 1379–1385. https://doi.org/10.1001/archneurol.2010.280.
Narayanan, S., Fu, L., Pioro, E., De Stefano, N., Collins, D.L., Francis, G.S., et al., 1997. Imaging of axonal damage in multiple sclerosis: spatial distribution of magnetic resonance imaging lesions. Ann. Neurol. 41 (3), 385–391. https://doi.org/10.1002/ana.410410314.
O'Rourke, M.F., Hashimoto, J., 2007. Mechanical factors in arterial aging: a clinical perspective. J. Am. Coll. Cardiol. 50 (1), 1–13. https://doi.org/10.1016/j.jacc.2006.12.050.
Park, H.J., Levitt, J., Shenton, M.E., Salisbury, D.F., Kubicki, M., Kikinis, R., et al., 2004. An MRI study of spatial probability brain map differences between first-episode schizophrenia and normal controls. Neuroimage 22 (3), 1231–1246. https://doi.org/10.1016/j.neuroimage.2004.03.009.
Petit-Taboue, M.C., Landeau, B., Desson, J.F., Desgranges, B., Baron, J.C., 1998. Effects of healthy aging on the regional cerebral metabolic rate of glucose assessed with statistical parametric mapping. Neuroimage 7 (3), 176–184. https://doi.org/10.1006/nimg.1997.0318.
Raz, N., Yang, Y., Dahle, C.L., Land, S., 2012. Volume of white matter hyperintensities in healthy adults: contribution of age, vascular risk factors, and inflammation-related genetic variants. Biochim. Biophys. Acta, Gen. Subj. 1822 (3), 361–369. https://doi.org/10.1016/j.bbadis.2011.08.007.
Ryu, W.S., Woo, S.H., Schellingerhout, D., Chung, M.K., Kim, C.K., Jang, M.U., et al., 2014. Grading and interpretation of white matter hyperintensities using statistical maps. Stroke 45 (12), 3567–3575. https://doi.org/10.1161/STROKEAHA.114.006662.
Schnack, H.G., van Haren, N.E., Hulshoff Pol, H.E., Picchioni, M., Weisbrod, M., Sauer, H., et al., 2004. Reliability of brain volumes from multicenter MRI acquisition: a calibration study. Hum. Brain Mapp. 22 (4), 312–320. https://doi.org/10.1002/hbm.20040.
Toga, A.W., Thompson, P.M., Mega, M.S., Narr, K.L., Blanton, R.E., 2001. Probabilistic approaches for atlasing normal and disease-specific brain variability. Anat. Embryol. (Berl.) 204 (4), 267–282. https://doi.org/10.1007/s004290100198.
Vermeer, S.E., Hollander, M., van Dijk, E.J., Hofman, A., Koudstaal, P.J., Breteler, M.M., et al., 2003. Silent brain infarcts and white matter lesions increase stroke risk in the general population: the Rotterdam Scan Study. Stroke 34 (5), 1126–1129. https://doi.org/10.1161/01.STR.0000068408.82115.D2.
Warntjes, J.B., Engström, M., Tisell, A., Lundberg, P., 2013. Brain characterization using normalized quantitative magnetic resonance imaging. PLoS One 8 (8), e70864. https://doi.org/10.1371/journal.pone.0070864.
Wen, W., Sachdev, P., 2004. The topography of white matter hyperintensities on brain MRI in healthy 60- to 64-year-old individuals. Neuroimage 22 (1), 144–154. https://doi.org/10.1016/j.neuroimage.2003.12.027.
Winblad, B., Palmer, K., Kivipelto, M., Jelic, V., Fratiglioni, L., Wahlund, L.O., et al., 2004. Mild cognitive impairment–beyond controversies, towards a consensus: report of the International Working Group on Mild Cognitive Impairment. J. Intern. Med. 256 (3), 240–246.
Yin, J.H., Song, Z.Y., Shan, P.F., Xu, J., Ye, Z.M., Xu, X.H., et al., 2012. Age- and gender-specific prevalence of carotid atherosclerosis and its association with metabolic syndrome in Hangzhou, China. Clin. Endocrinol. (Oxf.) 76 (6), 802–809. https://doi.org/10.1111/j.1365-2265.2011.04198.x.
Yoo, B.I., Lee, J.J., Han, J.W., Oh, S.Y., Lee, E.Y., MacFall, J.R., et al., 2014. Application of variable threshold intensity to segmentation for white matter hyperintensities in fluid attenuated inversion recovery magnetic resonance images. Neuroradiology 56 (4), 265–281. https://doi.org/10.1007/s00234-014-1322-6.
Yoshita, M., Fletcher, E., DeCarli, C., 2005. Current concepts of analysis of cerebral white matter hyperintensities on magnetic resonance imaging. Top. Magn. Reson. Imaging 16 (6), 399–407. https://doi.org/10.1097/01.rmr.0000245456.98029.a8.
Zhuang, F.J., Chen, Y., He, W.B., Cai, Z.Y., 2018. Prevalence of white matter hyperintensities increases with age. Neural Regen. Res. 13 (12), 2141–2146. https://doi.org/10.4103/1673-5374.241465.